FRP-Strengthening in Shear: Tests and Design Equations

by G. Monti and M.A. Liotta

<u>Synopsis:</u> This paper presents the results of an experimental/analytical study aiming at obtaining a clear understanding of the underlying mechanisms of the shear strengthening of reinforced concrete beams with fibre reinforced polymers (FRP). Through the definition of the generalised constitutive law of a bonded FRP sheet, of the compatibility imposed by the shear crack opening, and of the appropriate boundary conditions depending on the strengthening configuration, analytical expressions of the stress field in the FRP sheet crossing a shear crack are obtained. These expressions allow to easily define closed-form equations for the effective strength of FRP strips/sheets used for shear strengthening, as function of both the adopted strengthening configuration and some basic geometric and mechanical parameters. The FRP contribution is then added to those of concrete and steel. The equations accuracy has been verified through correlation studies with experimental results obtained from the literature and from laboratory tests on purposely under-designed real-scale beam specimens, strengthened with different FRP schemes.

Giorgio Monti is a Full Professor of Structural Engineering at the University "La Sapienza" of Rome. He is a member of the Commission Design of *fib* (fédération internationale du béton), in the groups "Seismic Concrete Design", "Computer-based Modelling and Design" and "Design of Structures Reinforced by FRP". His research interests span from reliability to the assessment and retrofitting of existing structures in seismic zones.

Marc'Antonio Liotta is a PhD student in Structural Engineering at the Structural and Geotechnical Engineering Department of the Università La Sapienza of Rome. His main interests are in FRP strengthened reinforced concrete members, behaviour of reinforced concrete structures and application of prestressed FRP fabrics on concrete members.

1. INTRODUCTION

In the development of practical and reliable design equations for shear strengthening of reinforced concrete elements with FRP composite materials, three aspects still remain not perfectly understood. The first regards the shear resisting mechanism that develops when FRP strips/sheets are side bonded, rather than U-jacketed or wrapped, to the element; in this case, a different mechanism than the Mörsch truss activates, that is, a "crack-bridging" mechanism, similar in nature to those of aggregate interlock, dowel effect and concrete tooth. The second aspect regards the evaluation of the contribution of the FRP transverse strengthening to the shear capacity: FRP is subjected to a variable tensile stress along the crack profile, which is conveniently expressed as an effective stress whose intensity is usually given through diagrams and not through closed-form equations. The third aspect regards the evaluation of the relative contributions to the shear capacity of concrete, steel and FRP at ultimate; it is not guaranteed that both concrete and stirrups can exploit their maximum strength when in the presence of FRP strengthening. The clarification of these aspects is the object of the present work, where they are treated from both the experimental and the analytical standpoint.

2. EXPERIMENTAL TESTS

Twenty-four beam specimens, purposely designed as under-reinforced in shear, were tested with a 3-point bending scheme (Monti et al. 2004). The concrete mean compressive cubic strength was R_{cm} = 13.3 MPa and the steel rebars had mean yield strength f_{ym} = 500 MPa. The geometric dimensions of the beams were: span 2.80 m, cross-section width 250 mm and depth 450 mm. The longitudinal reinforcement was made of 4ϕ20 bottom and of 2ϕ20 top, while shear stirrups ϕ8/400 mm were used. In view of the external strengthening application the bottom corners of the beam were rounded with 30 mm radius. All strips/sheets of the external strengthening were in a single layer of CFRP, having thickness 0.22 mm and elastic modulus E_f = 390 GPa. Figure 1 shows both the specimen's dimensions and loading scheme. The nomenclature used for each typology is represented in Table 1.

2.1   Tests description and results

REF1: Reference specimen, unstrengthened. Formation of the first cracks at 100 kN load. Progressive opening and formation of further cracks until failure. The failure was reached due to rupture of the second stirrup, at 550 mm from the left beam end, at 210 kN. Figure 3

REF2: Reference specimen, unstrengthened. Formation of the first cracks at 110 kN load. Failure reached due to rupture of the third stirrup, at 900 mm from the left beam end, at 187 kN.

SS90: Beam with S-strengthening, with CFRP strips 150 mm wide at $\beta = 90°$, with 300 mm spacing. The first cracks were observed at the load of 120-130 kN. The beam failure was reached at 200 kN. The reinforcement seemed to strengthen the beam very little, because the principal crack crossed the strips close to their end.

SS45: Beam with S-strengthening, with CFRP strips 150 mm wide at $\beta = 45°$, with 300 mm spacing, measured along the beam axis. The first cracks were observed at the load of 120/130 kN. At 170 kN the strip at right of midspan started to debond at the bottom. The beam failure was reached at 202 kN for complete delamination of the lower part of the second and third strip at the left of the beam.

SSVA: Beam with S-strengthening, with CFRP strips 150 mm wide with variable inclination (30°-45°-60°) and with spacing as in Figure 7. At 90 kN of load the first flexural cracks were noted. Around 140 kN debonding of the third strip from left of the beam started. Beam failure at 210 kN due to failure with complete debonding from the top of the 30°-strip.

SF90: Beam with S-strengthening, with CFRP sheets at $\beta = 90°$. At 208 kN debonding occurs at the beam midspan. At 213 kN first shear cracks observed. At 225 kN beam failure with rupture of the stirrup at 900 mm from the beam end.

US90: Beam with U-strengthening, with CFRP strips 150 mm wide at $\beta = 90°$, with 300 mm spacing. Failure was due to the rupture of the third stirrup, after debonding of the second strip from left occurred. The failure load of 190 kN was close to the unstrengthened beam because the strips were not activated.

US60: Beam with U-strengthening, with CFRP strips 150 mm wide at $\beta = 45°$, with 300 mm spacing, measured orthogonally to the strips. Formation of the first shear cracks at 135 kN. The third strip from left started to debond from the top at 165 kN. Debonding also started from the bottom at 199 kN, probably because of a crack at the beam soffit. Specimen failure at 222 kN, apparently without stirrup rupture.

USVA: Beam with U-strengthening, with CFRP strips 150 mm wide with variable inclination (30°-45°-60°) as in SSVA. Vertical flexural cracks at midspan around 100 kN of load. Slightly inclined cracks at midspan around 110 kN. Formation of shear cracks located between the strips at 30° and 45°**.** Specimen failure at 240 kN for debonding from the top of the 30° strip.

USV+: Beam with U-strengthening, with CFRP strips 150 mm wide with variable inclination (30°-45°-60°) as in USVA with a further bottom collaboration strip on the beam sides. Shear cracks around 170 kN. Debonding of the mid-span strip at the beam bottom. Specimen failure at 270 kN without stirrup rupture.

US45+: Beam with U-strengthening, with CFRP strips 150 mm wide at $\beta = 45°$, with 300 mm spacing, measured along the beam axis. At 100 kN first flexural cracks were observed. At 167 kN first shear cracks were observed. At 223 kN debonding of the

second strip from left started. At 232 kN debonding of the second strip from left started. Beam failure at 251 kN with complete debonding of the second strip.

   US90(2): Beam with U-strengthening, with CFRP strips 150 mm wide at β = 90°, with 300 mm spacing. At 90 kN first flexural cracks were observed. At 127 kN first shear cracks were observed. At 135 kN the third strip from left started to debond. At 166 kN debonding of the second strip from left. Failure at 179 kN, accompanied by opening of the stirrups hooks.

   UF90: Beam with U-strengthening, with CFRP sheets at β = 90°. First crack at 178 kN. Debonding starts at 206 kN. At 215 kN reinforcement buckling at the beam top, probably due to the upper concrete compression. Fabric failure around 250 kN and specimen failure at 260 kN with stirrups rupture.

   An information emerged from this first series of tests regards the limitation of the strips spacing. It has been verified that the strip spacing should be sufficiently close to avoid the formation of cracks that do not cross at least one strip. From Figure 16 it can be seen that, thinking to "condense" the strips in an "equivalent stirrup" on the strip axis, having the same height of the strip minus the effective bond length L_e from both ends in case of Side-bonding and only from one in case of U-Jacketing, shear cracks can develop that do not cross excessively spaced strips in the effective zone.

In fact, in the case of side bonding there exists a field, shown in Figure 8, where the crack, represented in its minimum and maximum inclination, can freely pass in between strips, without crossing and activating them. From the figure, it can be seen that such field reduces its extension passing from Side-bonding to U-jacketing and increasing the fibre inclination. This conclusion is supported by the observation of tests and from correlation of theoretical and experimental results shown in section 4 and suggests to adopt the following limitations in case of strip strengthening: the width w_f and the spacing p_f of the strips, measured (in mm) orthogonally with respect to the angle β of the fibre direction, should respect the following limitations: 50 mm $\leq w_f \leq$ 250 mm, $p_f \leq$ min$\{0.5\ d,\ 3\ w_f,\ w_f + 200\ \text{mm}\}$ and $p_f \geq 2\ w_f$. Obeying to these limitations a second series of beam tests was carried out.

   US45++: Beam with U-strengthening, with CFRP strips 50 mm wide at β = 45°, spacing 150mm along the beam axis. First crack at 184 kN. Failure of first strip at 261 kN and shear failure of beam at 267 kN.

   WS45++: Beam with W-strengthening, with CFRP strips 50 mm wide at β = 45°, spacing 150 mm along the beam axis. First crack at 182 kN. Failure of first strip at 291 kN and shear failure of beam at 317 kN.

   Ref3 and Ref4: Two more reference specimens to ensure the concrete strength of the second casting to be the same as the one in the first series of beams. Shear failure at 187 and 200 kN of load, respectively.

   US45+ "A": Beam with U-strengthening, with CFRP strips 150 mm wide at β = 45° with 225 mm spacing, measured along the beam axis. First crack at 184 kN. First shear cracks at 197 kN. Failure at 334,2 kN with stirrup overlap opening.

   US45++ "B": Beam with U-strengthening, with CFRP strips 150 mm wide at β = 45° with 225 mm spacing, measured along the beam axis. First crack at 184 kN.

US45++ "C": Beam with U-strengthening, with CFRP strips 150 mm wide at β = 45° with 225 mm spacing, measured along the beam axis. First shear cracks appear at 184 kN. First strip breaks at 288 kN. Strengthening failure around 364 kN and specimen failure at 366kN without stirrups rupture.

US45++ "F": Beam with U-strengthening, with CFRP strips 150 mm wide at β = 45° with 300 mm spacing, measured along the beam axis. Formation of first shear cracks between 204 and 212 kN. Shear failure at 300 kN, with stirrup overlap opening at one side and stirrup failure on the other side.

US45++ "E": Beam with U-strengthening, with CFRP strips 150 mm wide at β = 45° with 300 mm spacing, measured along the beam axis. Formation of first shear cracks at 210 kN. Shear failure at 327 kN, with stirrup overlap opening at one side and stirrup failure on the other side.

US45++ "D": Beam with U-strengthening, with CFRPstrips 150 mm wide at β = 45° with 300 mm spacing, measured along the beam axis. First crack at 210 kN. Shear failure at 229 kN, with stirrup overlap opening at one side and stirrup failure on the other side.

3. DESIGN EQUATIONS FOR FRP SHEAR STRENGTHENING

This section tries to provide a coherent analytical framework to describe the behaviour of RC elements FRP-strengthened in shear, following previous efforts made by other authors (Täljsten 1997, Triantafillou 1998, Khalifa et al. 1998). The developed theory aims at describing the FRP stress distribution $\sigma_{f,cr}(x)$ along a shear crack (as qualitatively sketched in Figure 27) through closed-form equations, as opposed to regression-based formulas (Triantafillou & Antonopoulos 2000). Once this is correctly defined, the FRP resultant across the crack can be computed and the FRP contribution to the resisting shear be found. The analytical developments arrive at defining three predictive equations for: Side Bonding (S), U-jacketing (U) and Wrapping (W).

The obtained expressions of the strength are given in terms of readily available geometrical and mechanical quantities of both the FRP strengthening and the RC beam and are then used to compute the FRP contribution to the overall shear strength, together with that of concrete and transverse reinforcement. These equations have been adopted in the new Code for FRP strengthening recently issued by the Italian Research Council (CNR 2005)

In the following developments, the following hypotheses are made (notation in Figure 28):

- Shear cracks are evenly spaced along the beam axis, and inclined with angle θ,
- At the ULS the cracks depth is equal to the internal lever arm $z = 0.9\,d$,
- In the case of U-jacketing (U) and wrapping (W), the resisting shear mechanism is based on the Moersch truss, while in the case of side bonding (S), because the Moersch truss cannot form as the tensile diagonal tie is missing, a different resisting mechanism of "crack-bridging" is considered to develop.

In order to fully characterize the physical phenomenon, the following aspects must be analytically defined: a) the failure criterion of an FRP strip/sheet bonded to concrete, b)

the stress-slip constitutive law, c) the compatibility equations (*i.e.*, the crack opening), and d) the boundary conditions (*i.e.*, the available bonded lengths on both sides of the crack depending of the different configurations).

3.1   Generalised failure criterion of an FRP strip/sheet bonded to concrete

The criterion includes the two cases of: a) straight strip/sheet, and b) strip/sheet wrapped around a corner. Two quantities are introduced: the *effective bond length* l_e and the *debonding strength* $f_{fdd}(L)$, expressed as function of the available bond length l_b.
The effective bond length (optimum anchorage length) is given as:

$$l_e = \sqrt{\frac{E_f t_f}{2 f_{ctm}}} \quad [\text{length in } mm] \tag{1}$$

where: E_f = FRP sheet elastic modulus, t_f = sheet thickness, $f_{ctm} = 0.27 \cdot R_{ck}^{2/3}$ = concrete mean tensile strength (with R_{ck} = concrete characteristic cubic strength).
The specific rupture energy Γ_{Fk} of the concrete-strngthening bond can be expressed as:

$$\Gamma_{Fk} = 0.03 \cdot k_b \cdot \sqrt{f_{ck} \cdot f_{ctm}} \text{ ,[units: } N, mm] \tag{2}$$

where f_{ck} is the concrete characteristic cubic strength and k_b = covering/scale coefficient (Brosens and Van Gemert 1999), given as:

$$k_b = \sqrt{\frac{2 - w_f / p_f}{1 + w_f / 400}} \geq 1 \tag{3}$$

where, for strips: w_f = width measured orthogonally to β, p_f = spacing measured orthogonally to β; while for sheets $k_b=1$. Note however that w_f should not exceed $\min(0.9d, h_w) \cdot \sin(\theta+\beta)/\sin\theta$, with d = beam effective depth, h_w = beam web depth, β = angle of strip/sheet to the beam axis, θ = crack angle to the beam axis.
The debonding strength is given as:

$$f_{fdd} = \frac{0.80}{\gamma_{f,d}} \sqrt{\frac{2 E_f \Gamma_{Fk}}{t_f}} \quad \text{units: } [N, mm] \tag{4}$$

where $\gamma_{f,d}$ is a partial safety factor depending on the application accuracy. In case the available bond length l_b is lower than the optimum anchorage length, l_e, the design strength should be reduced to the value $f_{fdd,rid}$ given as:

$$f_{fdd,rid} = f_{fdd} \cdot \frac{l_b}{l_e} \left(2 - \frac{l_b}{l_e} \right). \tag{5}$$

The ultimate strength of the FRP strip/sheet, which includes the case when it is wrapped around a corner rounded with a radius r_c, is:

$$f_{fu}(l_b, \delta_e, r_c) = f_{fdd}(l_b) + \left\langle \phi_R \cdot f_{fu} - f_{fdd}(l_b) \right\rangle \cdot \delta_e, \quad \text{where:}$$

$$\delta_e = \begin{cases} 0 & \text{free end} \\ 1 & \text{end around a corner} \end{cases} \tag{6}$$

where it can be seen that the debonding strength depends on the available bonded length l_b and $\langle \cdot \rangle$ denotes that the bracketed expression is zero if negative. It is noted that the sheet wrapped around a corner attains a fraction ϕ_R of the ultimate strength f_{fu} of the FRP sheet depending on the coefficient ϕ_R as function of the rounding radius r_c with respect to the beam width b_w (Campione and Miraglia 2003):

$$\phi_R = 0.2 + 1.6\, \frac{r_c}{b_w}, \qquad 0 \le \frac{r_c}{b_w} \le 0.5 \tag{7}$$

When $l_b \ge l_e$, the expression for the ultimate strength of the FRP strip/sheet, wrapped around a corner with a radius r_c, becomes:

$$f_{fu,W}(r_c) = f_{fdd} + \left\langle \phi_R \cdot f_{fu} - f_{fdd} \right\rangle \tag{8}$$

3.2   Generalised stress-slip constitutive law

The generalised stress-slip law $\sigma_f\,(u,l_b,\delta_e)$ of FRP strips/sheets bonded to concrete, including both cases of free end or wrapped around a corner, is shown in Figure 29.

3.3   Compatibility (crack width)

Considering a reference system with the origin fixed at the upper limit of the shear crack and with abscissa x along the crack itself (Figure 31), the crack width (normal to the crack axis) along the shear crack can be expressed as $w = w(x)$.

3.4   Boundary conditions (available bond length)

The boundary conditions refer to the available bond length $L(x)$ on both sides of the shear crack and should be defined according to the strengthening scheme adopted: either S=Side bonding, U=U-jacketing, W=Wrapping (Figure 31).

3.5   FRP stress profile along the shear crack

In order to obtain the stress profile in the FRP sheet along the crack as a function of both the crack opening and the available bond length on both sides of the crack itself, one has to substitute into the constitutive law $\sigma_f\,(u,l_b,\delta_e)$: a) the compatibility equation $u = u(\alpha, x)$, b) the boundary condition $l_b = l_b(x)$ given according to the strengthening configuration, and c) the end constraint given by the appropriate value of δ_e. Figure 32 qualitatively depicts the $\sigma_{f,cr}(x)$ profiles along the crack for the three different strengthening configurations considered, when sheets are used. In the configuration S, the stress profile is truncated towards the end of the crack, where the available length tends to zero. In the configuration U, the stress profile remains constant where the available length allows the full debonding strength to be developed throughout the crack length. In the configuration W, the stress profile rises towards the end of the crack, where, after

complete debonding, the sheet is restrained at both ends and subjected to simple tension up to its tensile strength.

3.6   Determination of FRP contribution to the shear strength

The objective is to obtain the maximum contribution of the FRP strips/sheet to the shear strength. This means to identify, among all possible shapes of the FRP stress profile $\sigma_{f,cr}[u(\alpha,x),l_b(x)]$, which changes with the crack opening α, the one offering the maximum contribution.

3.6.1 Effective stress in the FRP sheet -- To this aim it is expedient to define an effective stress in the FRP sheet, inclined to an angle β as the FRP fibres, as the mean FRP stress field $\sigma_{f,cr}(x)$ along the shear crack length $z/\sin\theta$:

$$\sigma_{fe}(\alpha) = \frac{1}{z/\sin\theta} \cdot \int_0^{z/\sin\theta} \sigma_{f,cr}[u(\alpha,x),l_b(x)]\,dx \tag{9}$$

which might be regarded as an equivalent constant FRP stress block along the shear crack.

3.6.2 Effective debonding strength -- The maximum of the FRP effective stress, which is termed the effective debonding strength f_{fed}, is found by imposing:

$$\frac{d\sigma_{fe}[x_u(\alpha)]}{d\alpha} = \frac{d\sigma_{fe}(x_u)}{dx_u} \cdot \frac{dx_u(\alpha)}{d\alpha} = 0 \tag{10}$$

where the chain rule has been used. Solution of (10) allows to determine the FRP stress profile with the maximum area, that is, the effective strength of the FRP shear strengthening.
In the case of side-bonding (however, not allowed for seismic strengthening):

$$f_{fed} = f_{fdd} \cdot \frac{z_{rid,eq}}{\min\{0.9\,d,h_w\}} \cdot \left(1 - 0.6\sqrt{\frac{l_{eq}}{z_{rid,eq}}}\right)^2 \tag{11}$$

where :

$$z_{rid,eq} = z_{rid} + l_{eq}, \quad z_{rid} = \min\{0.9\,d,h_w\} - l_e \cdot \sin\beta, \quad l_{eq} = \frac{s_f}{f_{fdd}/E_f} \cdot \sin\beta \tag{12}$$

and it is observed that: z_{rid} is equal to the minimum between the effective depth of the section (that is equal to the vertical projection of the crack) minus the bottom part where there is not enough bond length and the beam web in case of T sections, l_{eq} is the bonded length projected vertically that would be necessary if the fabric strain $\varepsilon_{fdd} = f_{fdd}/E_f$ was uniform and s_f is the slip at debonding.

In the case of U-jacketing:

$$f_{fed} = f_{fdd} \cdot \left[1 - \frac{1}{3} \frac{l_e \sin \beta}{\min\{0.9\,d, h_w\}} \right] \tag{13}$$

In the case of wrapping:

$$f_{fed} = f_{fdd} \cdot \left[1 - \frac{1}{6} \frac{l_e \sin \beta}{\min\{0.9\,d, h_w\}} \right] + \frac{1}{2}(\phi_R \cdot f_{fd} - f_{fdd}) \cdot \left[1 - \frac{l_e \sin \beta}{\min\{0.9\,d, h_w\}} \right] \tag{14}$$

where f_{fd} is the design ultimate strength of the FRP to be evaluated as in

$$f_{fu,W}(r_c) = f_{fdd} + \langle \phi_R \cdot f_{fu} - f_{fdd} \rangle \tag{15}$$

In the previous equation the second term should be considered only when positive.

3.7   Shear capacity with FRP

In case the reinforcement type is U or W, the Moersch resisting mechanism can be activated and the shear carried by FRP is expressed as:

$$V_{Rd,f} = \frac{1}{\gamma_{Rd}} \cdot 0.9\,d \cdot f_{fed} \cdot 2 t_f \cdot (\cot \theta + \cot \beta) \cdot \frac{w_f}{p_f} \tag{16}$$

while for side-bonding (S) the FRP role is that of "bridging" the shear crack, so that:

$$V_{Rd,f} = \frac{1}{\gamma_{Rd}} \cdot \min\{0.9\,d, h_w\} \cdot f_{fed} \cdot 2 t_f \cdot \frac{\sin \beta}{\sin \theta} \cdot \frac{w_f}{p_f} \tag{17}$$

with d = beam effective depth, f_{fed} = design effective strength of the FRP shear strengthening, given either by (11) for side bonding or by (13) for U-jacketing or by (14) for wrapping, t_f = thickness of FRP strip/sheet (on single side) with angle β, θ = crack angle, s_f, w_f = strip spacing and width, respectively, measured orthogonally to the fibre direction β.

Assuming cracks inclined of an angle $\theta = 45°$ with respect to the vertical and strips/sheets vertically aligned at $\beta = 90°$, the two previous equations become:

$$V_{Rd,f} = \frac{1}{\gamma_{Rd}} \cdot 0.9\,d \cdot f_{fed} \cdot 2 t_f \cdot \frac{w_f}{p_f} \tag{18}$$

$$V_{Rd,f} = \frac{1}{\gamma_{Rd}} \cdot \min\{0.9\,d, h_w\} \cdot f_{fed} \cdot 2 t_f \cdot \sqrt{2} \frac{w_f}{p_f} \tag{19}$$

The shear verification should be performed by comparing the design acting shear with the shear capacity, given by:

$$V_{Rd} = \min\{ V_{Rd,ct} + V_{Rd,s} + V_{Rd,f}, V_{Rd,\max} \} \tag{20}$$

where $V_{Rd,ct}$ is the concrete contribution, given by (*e.g.*, EC2 (CEN 1991), not accounted for):

$$V_{Rd,ct} = \frac{0.18}{\gamma_c} b_w \cdot d \cdot \min\left\{1+\sqrt{\frac{200 \text{ mm}}{d}}, 2\right\} \cdot \sqrt[3]{100 \cdot \min\{0.02, \rho_{sl}\} \cdot f_{ck}} \qquad (21)$$

and $V_{Rd,s}$ is the steel contribution, given by:

$$V_{Rd,s} = 0.9\,d \cdot f_{yd} \frac{n_{st} \cdot A_{st}}{s_{st}} (\cot\theta + \cot\beta_{st}) \sin\beta_{st} \qquad (22)$$

where $f_{ctd} = 0.7\,f_{ctm}/\gamma_c$ = concrete tensile strength, $\gamma_c = 1.5$ = concrete partial coefficient, b_w = web section width, ρ_{sl} = longitudinal geometric ratio, f_{ck} = concrete characteristic cylindrical strength, f_{yd} = design steel yield strength, n_{st} = transverse reinforcement arm number, A_{st}, s_{st} = area (one arm) and spacing of traverse reinforcement, e β_{st} = stirrups angle.

In (20), $V_{Rd,max}$ is the strength of the concrete strut, given by (*e.g.*, EC2):

$$V_{Rd,max} = 0.9d \cdot b_w \cdot \nu \cdot f_{cd} \cdot (\cot\theta + \cot\beta_{st})/(1+\cot^2\theta) \qquad (23)$$

with $\qquad\qquad\qquad\qquad \nu = 0.6[1 - f_{ck}/250] \quad [\text{in MPa}]. \qquad (24)$

VALIDATION OF DESIGN EQUATIONS

The results obtained with the above presented equations are both applied to the case of the specimen beams tested in the lab and to other authors' test specimens; the results are shown in Figure 33, also in comparison with the results obtained following the ACI 440 code (ACI 440.2R-02).. Partial coefficients were set to 1 for the prediction of experimental results, and material properties were considered with their mean values. In the equations for the variable inclination reinforcements a mean value of the strips inclinations is considered, while spacing is the effective one. The shear capacity of the reference beam was computed as the mean between the two tested unstrengthened specimens. Please note that in the specimen SS90, SS45, and US90, the contribution of FRP strengthening was not considered, as it was recognised that the diagonal shear cracks did not cross the strips.

It can be observed that the mean error on the predictions that activated the FRP strengthening is 7%, with a peak of 15% for the configurations US60 and UF90. Such an error can be considered as acceptable. Further tests are being carried out to validate the proposed equations on different reinforcing schemes.

The work presented here addressed some of the still unsolved aspects in previous analytical treatments of shear strengthening of beams with composite materials (FRP) and proposes possible solutions for them. In particular, closed-form analytical

expressions for the effective strength of FRP strips/sheets crossing the shear crack were found, which are then introduced in design equations for the contribution of FRP to the shear strength of RC elements. In this respect, it has been clarified that the FRP contribution to the shear strength should be computed for U and W configurations with equation (16), based on the formation of the Moersch truss, while for S configurations equation (17) should be used instead, which considers the "bridging" of cracks. The equations developed showed good correlation with purposely carried out experimental tests. The equations matched the shear capacity increase with a more than acceptable error.

4. ACKNOWLEDGEMENTS

REFERENCES

ACI 440.2R-02 (2002). Guide for the Design and Construction of Externally Bonded FRP Systems for Strengthening Concrete Structures. *American Concrete Institute, Committee 440*

Brosens, K., and Van Gemert, D. (1999). Anchorage design for externally bonded carbon fiber reinforced polymer laminates. *Proc. 4th Int. Symposium on FRP Reinforcement for Concrete Structures*, Baltimore, USA, pp. 635-645.

Campione, G., and Miraglia, N. (2003). "Strength and strain capacities of concrete compression members reinforced with FRP". Cement and Concrete Composites, Elsevier, 25, 31-41.

CEN (1991). Eurocode 2: Design of concrete structures – Part 1-1: General rules and rules for buildings. ENV 1992-1-1, Comité Européen de Normalisation, Brussels, Belgium.

CNR (2005). Instructions for Design, Execution and Control of Strengthening Interventions with FRP. *Consiglio Nazionale delle Ricerche, Roma, Italy.*

fib (2001). Design and Use of Externally Bonded FRP Reinforcement (FRP EBR) for Reinforced Concrete Structures. *Bulletin no. 14, fib Task Group 9.3 'FRP Reinforcement for Concrete Structures'.*

Khalifa, A., Gold, W. J., Nanni, A. and Aziz, A. M. I. (1998). Contribution of externally bonded FRP to shear capacity of rc flexural members. *ASCE Journal of Composites for Construction*, 2(4), 195-202.

Monti, G., Santinelli, F., and Liotta, M.A. (2004). Shear strengthening of beams with composite materials. *Proc. 2nd International Conference on FRP Composites in Civil Engineering CICE 2004*, Adelaide, Australia, December.

Täljsten B. (1997). Strengthening of concrete structures for shear with bonded CFRP-fabrics. *Recent advances in bridge engineering, Advanced rehabilitation, durable materials, nondestructive evaluation and management*, Eds. U. Meier and R. Betti, Dübendorf, 57-64.

Triantafillou, T. C. (1998). Shear strengthening of reinforced concrete beams using epoxy-bonded FRP composites. *ACI Structural Journal*, 95(2), March-April, 107-115.

Triantafillou, T. C. and Antonopoulos, C. P. (2000). Design of concrete flexural members strengthened in shear with FRP. *ASCE Journal of Composites for Construction*, 4(4), 198-205.

Table 1. Typology, nomenclature and experimental shear strength of the tested beams.

STRENGTH'G APPLICATION	STRENGTH'G TYPE	FIBRES ANGLE	NAME	STRENGTHENING CONFIGURATION	EXP. SHEAR STRENGTH (kN)
	NONE	-	REF		95.0
SIDE BONDING	STRIPS width 150 mm spacing 300 mm	90°	SS90*		100.0
		45°	SS45		101.0
		60°, 45°, 30°	SSVA		105.0
	SHEETS	90°	SF90		112.5
U-JACKETING	STRIPS width 150 mm spacing 300 mm	90°	US90*		95.0
		60°	US60		111.0
		60°, 45°, 30°	USVA		120.0
		60°, 45°, 30°	USVA+		135.0
		45°	US45+		126.0
		90°	US90(2)*		90.0
	SHEETS	90°	UF90		125.0
	STRIPS, width 50mm spacing 100 mm		US45++		133.5
	SHEETS		UF45+ A		158.5
			UF45++B		167.0
			UF45++C		172.0
	STRIPS width 150 mm spacing 225 mm		US45++F		182.85
			US45++E		150.15
			US45+ D		163.45
WRAPPING	STRIPS width 50mm spacing 100 mm		WS45++		114.5

* In these tests, the shear cracks did not fully activate the FRP strips, which then did not contribute to the shear strength.
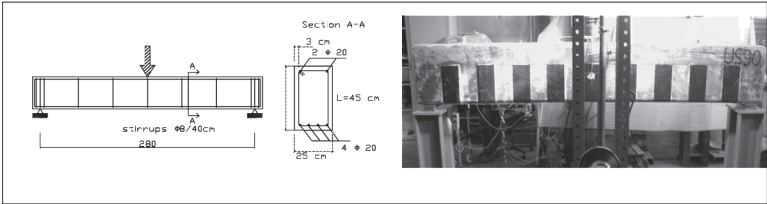
Figure 1 — Reference specimen dimensions and loading scheme (left) and representative picture of a test (right).

Figure 2 — Reference specimen REF1

Figure 3 — Reference specimen REF2
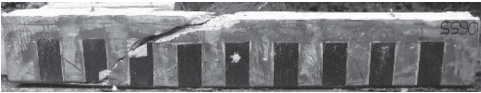
Figure 4 — Specimen SS90

Figure 5 — Specimen SS45

Figure 6 — Specimen SSVA
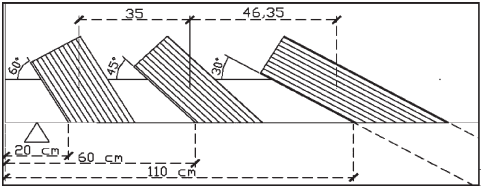
Figure 7 — Configuration of SSVA strengthening.
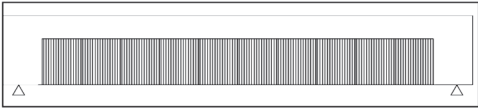
Figure 8 — Specimen SF90

Figure 9 — Specimen US90

Figure 10 — Specimen US60

Figure 11 — Specimen USVA

Figure 12 — Specimen USV+

Figure 13 — Specimen US45+

Figure 14 — Specimen US90

Figure 15 — Specimen UF90
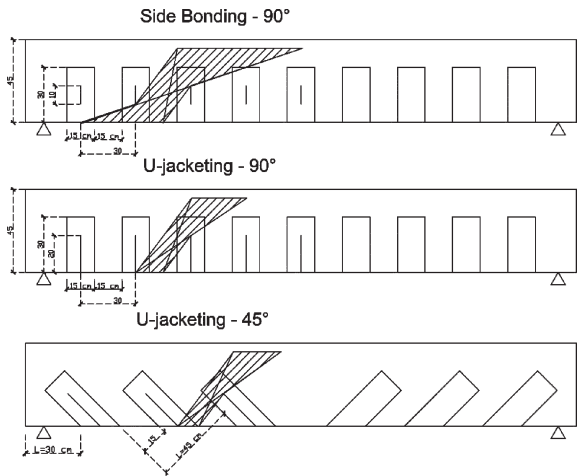
Figure 16 — Crack formation fields with inadequate strip spacing.

Figure 17 — Specimen US45+

Figure 18 — Specimen WS45+
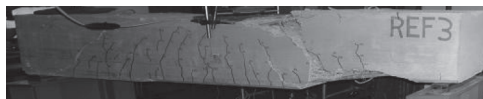
Figure 19 — Specimen REF3
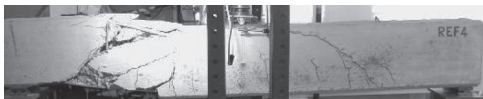
Figure 20 — Specimen REF4

Figure 21 — Specimen US 45+ "A"
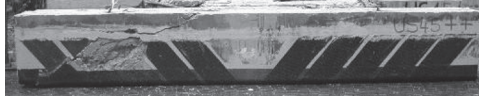
Figure 22 — Specimen US45++"B"

Figure 23 — Specimen US45++"C"

Figure 24 — Specimen US45++"F"

Figure 25 — Specimen US45++"E"
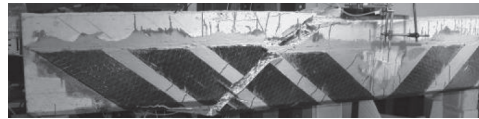
Figure 26 — Specimen US45++"D"
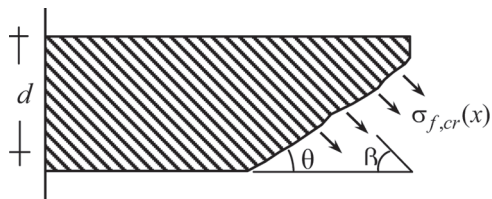
Figure 27 — Stress distribution along an FRP sheet crossing a shear crack.
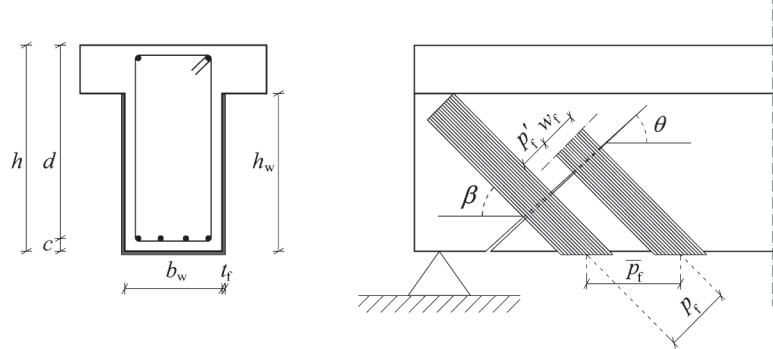
Figure 28 — Geometry notation.
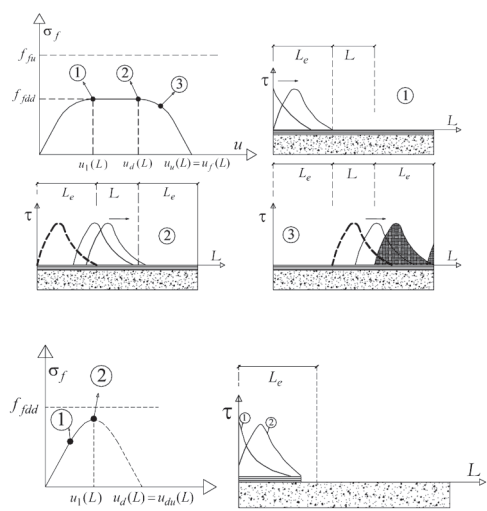
Figure 29 — Stress-slip law for the case of FRP strip/sheet with free end and with sufficient bond length (Top), and with small bond length (Bottom).
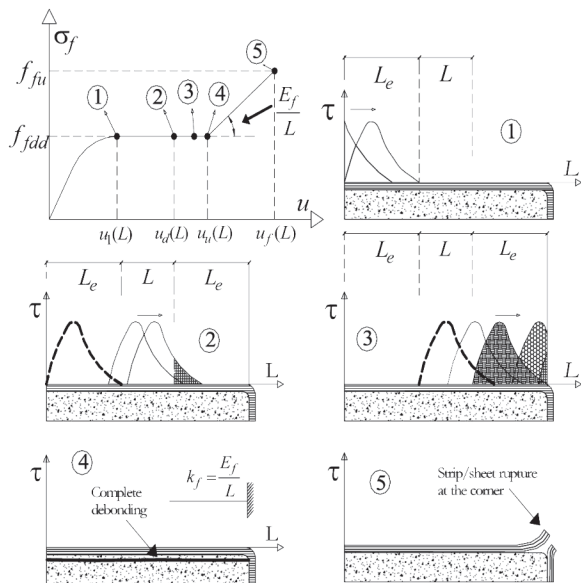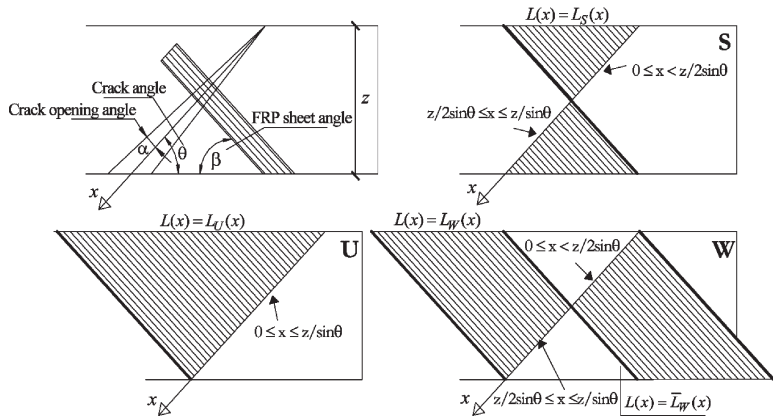
Figure 30 — Stress-slip law for the case of FRP strip/sheet wrapped around a corner.

Figure 31 — Boundary conditions (available bond length) for three strengthening configurations: S = Side bonding, U = U-jacketing, and W = Wrapping.
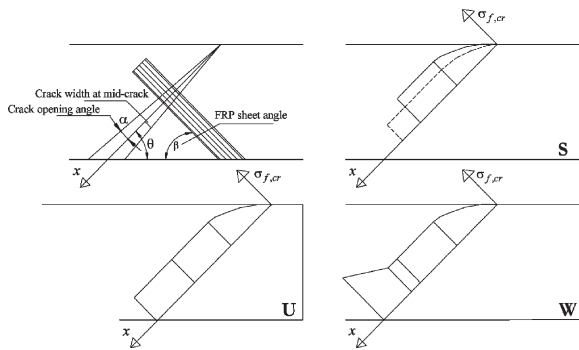
Figure 32 — Typical stress profiles in FRP sheets along the shear crack for three strengthening configurations: S = Side bonding, U = U-jacketing, and W = Wrapping.
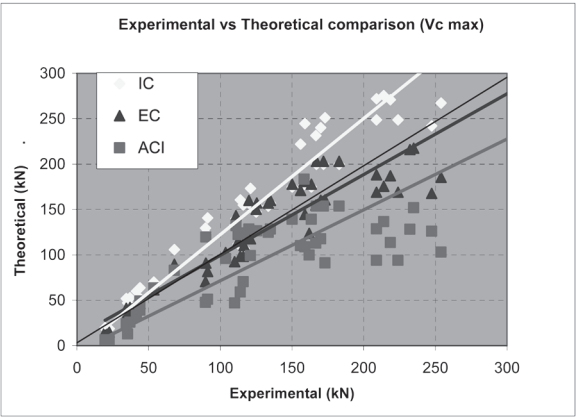

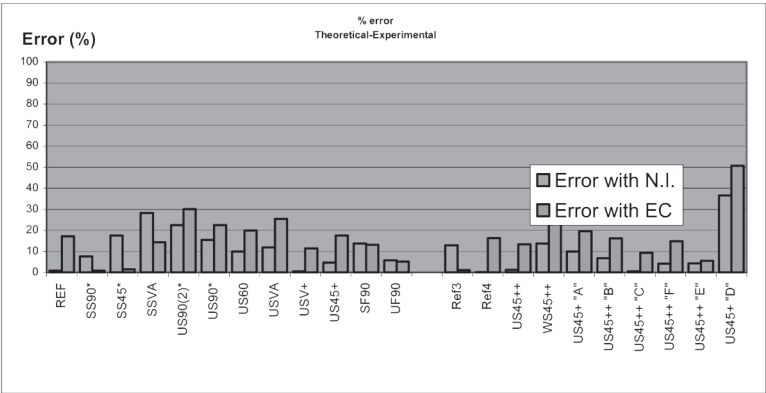Figure 33 — Prediction-test results comparison.

Figure 34 —Prediction-test results error.